Laser-induced adiabatic alignment of molecules dissolved in helium nanodroplets

Dominik Pentlehner,[1] Jens H. Nielsen,[2,*] Lars Christiansen,[2] Alkwin Slenczka,[3] and Henrik Stapelfeldt[1,4]
[1]*Department of Chemistry, Aarhus University, 8000 Aarhus C, Denmark*
[2]*Department of Physics and Astronomy, Aarhus University, 8000 Aarhus C, Denmark*
[3]*Institut für Physikalische und Theoretische Chemie, Universität Regensburg, 93040 Regensburg, Germany*
[4]*Interdisciplinary Nanoscience Center (iNANO), Aarhus University, 8000 Aarhus C, Denmark*
(Received 11 January 2013; published 4 June 2013)

A moderately intense, nonresonant, linearly polarized nanosecond laser pulse is used to induce one-dimensional (1D) adiabatic alignment of 1,4 diiodobenzene ($C_6H_4I_2$), iodobenzene (C_6H_5I), and methyliodide (CH_3I) molecules dissolved in helium nanodroplets. The alignment sharpens as the laser intensity is increased, similar to the behavior in gas phase. For diiodobenzene the highest degree of alignment, $\langle\cos^2\theta_{2D}\rangle = 0.90$, is essentially identical to the value obtained for isolated molecules in a supersonic beam, whereas the highest degrees of alignment for iodobenzene and for methyliodide in helium droplets fall below the values obtained for isolated molecules. We believe this is due to the deviation from axial recoil in the Coulomb explosion process that probes the alignment of the molecules in the He droplets.

DOI: 10.1103/PhysRevA.87.063401 PACS number(s): 37.10.Vz, 33.80.−b, 32.80.Rm, 42.50.Hz

I. INTRODUCTION

Laser-induced alignment, the method used to confine the principal (polarizability) axes of molecules along axes fixed in the laboratory frame by means of moderately intense laser pulses, has exploded in scope and application since the first theoretical and experimental papers heralded its advent in the last part of the 1990's [1–4]. It has been established that, overall, alignment occurs in the adiabatic or the nonadiabatic limit where the laser pulse is much longer or shorter, respectively, than the classical rotational period(s) of the molecules [5]. The nonadiabatic approach distinguishes itself by the ability to produce alignment after the turn-off of the laser pulse, i.e., under field-free conditions, which has proven most useful in many applications involving ultrashort laser pulses [6–8]. In the adiabatic approach alignment only occurs during the pulse but it offers, on the other hand, unsurpassed high degrees of alignment, straightforward generalization of one-dimensional (1D) (single axis) to three-dimensional (3D) alignment, and extension to tight orientational (head-versus-tail) control. These properties have also been exploited in a number of applications [9,10].

With the exception of a few papers [11–17] all work to date has treated the alignment of isolated gas phase molecules, although the extension to molecules in a solvent is of great interest, notably because most chemical reactions occur in a solvent rather than in the gas phase. A classical solvent may, however, be polarized or even ionized by the alignment laser, which can perturb any alignment created—as can the frequent collisions between the solvent molecules and the solvated molecules. Furthermore, a low rotational temperature T_{rot} of the molecules and their ability to rotate freely are prerequisites for achieving sharp alignment—conditions which are not provided by classical solvents. By contrast, molecules dissolved in the quantum fluid of a superfluid helium droplet are, according to spectroscopic observations [18–20], cooled to $T_{rot} = 0.38$ K and able to rotate freely. In Ref. [21] we already demonstrated 1D nonadiabatic laser alignment of molecules in helium droplets, and showed that the alignment dynamics differs strongly from the gas phase behavior. Here we report experimental studies of 1D adiabatic alignment of molecules dissolved in helium nanodroplets showing high degrees of alignment and pronounced similarities to the adiabatic alignment of isolated molecules.

II. EXPERIMENTAL SETUP

A schematic of the experimental setup is displayed in Fig. 1. The He droplets are formed by continuously expanding ∼20 atm He gas, cryogenically precooled to 10–20 K, through a 5 μm orifice into vacuum. The average size of the droplets is determined by the temperature of the He gas and is $\sim 1.1 \times 10^4$ helium atoms per droplet at 12 K [18] used in our measurements. The droplet beam passes through a pickup cell, where the partial pressure of $C_6H_4I_2$, C_6H_5I, or CH_3I is adjusted to optimize for single molecule doping of each droplet. Hereafter, the doped He droplet beam enters the target region where it is crossed, at 90°, by two collinear propagating pulsed laser beams. One laser beam, consisting of linearly polarized 10-ns-long [full width at half maximum (FWHM)] pulses from a Nd:YAG laser (YAG pulses: $\lambda = 1064$ nm), is used to align the molecules. The second laser beam, consisting of linearly polarized 30-fs-long (FWHM) pulses (probe pulses: $\lambda = 800$ nm) is used to probe the molecular orientation. These pulses are sufficiently intense ($I_{probe} = 1.8 \times 10^{14}$ W/cm^2) to multiply ionize either the $C_6H_4I_2$, C_6H_5I, or the CH_3I molecules resulting in Coulomb explosion into positively charged fragments, notably I^+ with a charged partner ion. Assuming that these I^+ ions recoil along the C-I bond axis (axial recoil approximation) of the parent molecule and by detecting their emission direction with a velocity map ion imaging spectrometer, the spatial orientation of the C-I bond axis of $C_6H_4I_2$, C_6H_5I, and CH_3I can be determined at the time of the probe pulse [22]. By electronically synchronizing the probe pulse to the peak of the YAG pulse, the spatial orientation of the molecules is probed at the time where the

*Present address: University College London, London, United Kingdom.

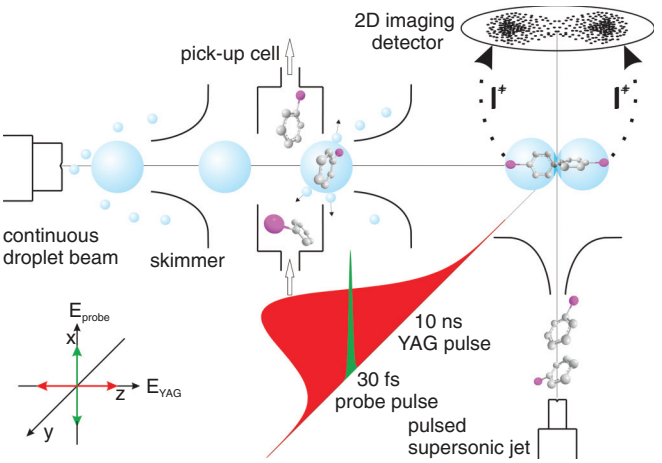

FIG. 1. (Color online) Schematic of the key elements in the experiment. The electrostatic plates projecting the ions onto the imaging detector are not shown. The polarization state of the YAG and the probe laser pulses are shown in the coordinate system and indicated by the pulses.

degree of alignment is highest [4]. To enable comparison of laser-induced alignment of molecules in He droplets and of isolated molecules under identical laser pulse conditions, the experimental apparatus is designed such that a second molecular beam, consisting of isolated $C_6H_4I_2$, C_6H_5I, or CH_3I molecules, can be sent into the target region. All experiments are conducted at 20 Hz, limited by the repetition rate of the YAG laser.

III. EXPERIMENTAL RESULTS

A. Ion images

Examples of ion images are shown in Fig. 2. For the isolated $C_6H_4I_2$ molecules, row (a), it is seen that when only the probe pulse, linearly polarized perpendicular to the two-dimensional (2D) imaging detector, is used, the I^+ image is circularly symmetric as expected for randomly oriented molecules. When the YAG pulse is included the I^+ ions tightly localize along its polarization axis—parallel to the detector plane (vertical in the figure). These observations show that the symmetry axis, containing the C-I bonds, of the diiodobenzene molecules is aligned along the YAG pulse polarization axis. It is the expected result since a linearly polarized laser pulse will align the most polarizable axis, which coincides with the C-I bond axis, along its polarization axis [5]. These findings are completely in line with previous studies of 1D adiabatic alignment of diiodobenzene (and other) molecules [23]. The two pairs of distinct, radially separated rings correspond to specific Coulomb explosion channels where the I^+ ions in the outermost (innermost) channel are formed as a result of Coulomb fragmentation of a triply (doubly) charged $C_6H_4I_2$ cation [22].

Next, we turn to the IHe^+ images from $C_6H_4I_2$ molecules embedded in He droplets [row (b)]. The reason for detecting IHe^+ rather than I^+ is that I^+ ion images may contain a small contribution from unsolvated molecules drifting from the pickup cell to the target region. Although the experimental setup is designed to make this contribution very small, the

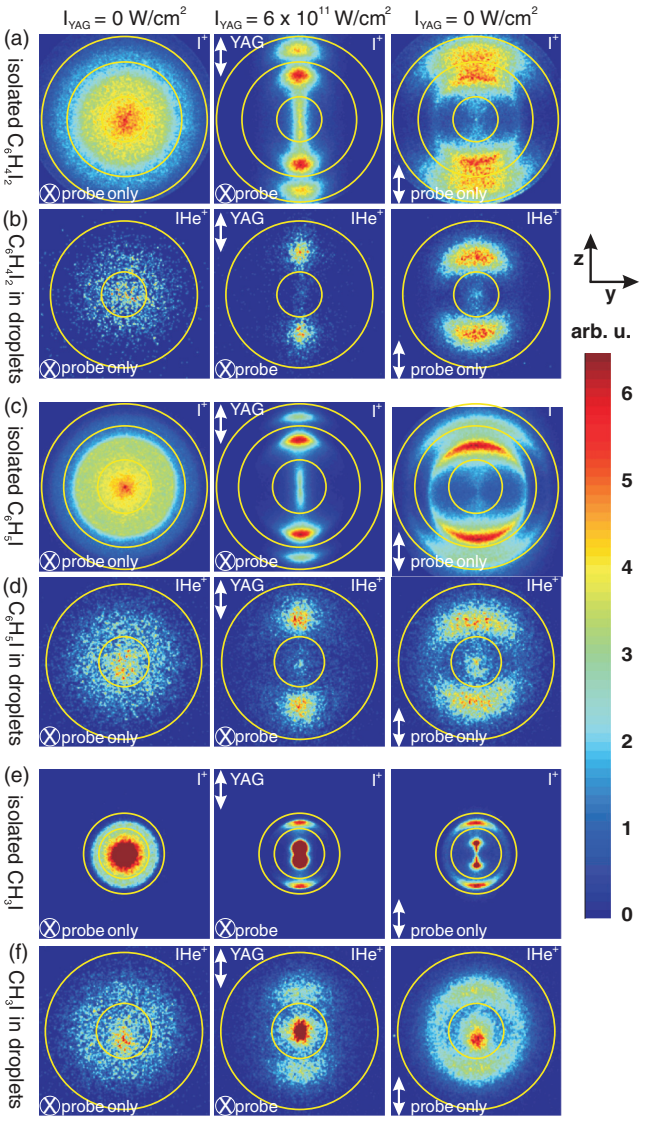

FIG. 2. (Color online) False color ion images from Coulomb explosion of $C_6H_4I_2$ [rows (a) and (b)], C_6H_5I molecules [rows (c) and (d)], and CH_3I molecules [rows (e) and (f)] recorded with the probe and YAG pulse polarizations as indicated. The color scale at the side indicates the relative number of ions. The circles indicate the radial ranges used for calculating $\langle\cos^2\theta_{2D}\rangle$. $I_{probe} = 1.8 \times 10^{14}$ W/cm^2 [24]. The velocity space in the gas phase and droplet experiment is the same for each molecule, but different for $C_6H_4I_2$ as compared to the others.

detection of IHe^+ ions ensures background-free conditions. We observed that IHe^+ ions carry the same angular information as the I^+ ions, justifying the use of IHe^+ ions as observables. Similar to the isolated molecule data, it is seen that the circular symmetry in the probe-only image changes to pronounced localization of ions along the polarization axis of the YAG pulse when it is included. These findings show 1D adiabatic alignment of molecules dissolved in He nanodroplets. Comparing rows (a) and (b) it is obvious that there are also some differences between the gas phase and the He droplet images. Notably, in the droplet image the two Coulomb explosion

channels observed in the isolated molecule case are replaced by only a single channel.

The corresponding results for iodobenzene are shown in rows (c) and (d) of Fig. 2. For the isolated molecules the ion images exhibit characteristics very similar to those observed for diiodobenzene, i.e., two distinct Coulomb explosion channels and tight localization of the I^+ ions along the YAG polarization [middle panel in row (c)], demonstrating tight alignment of the axis containing the C-I bond. The droplet image recorded with the YAG pulse included [middle panel in row (d)] is, however, more blurred than the corresponding isolated molecule image, demonstrating an apparently lower degree of alignment.

The results obtained for CH_3I molecules are shown in rows (e) and (f) of Fig. 2. For CH_3I the most polarizable axis is also the C-I axis and, therefore, we expect that the YAG pulse will confine this molecular axis along its polarization axis. The ion images, which probe the spatial orientation of the C-I axis, show that this is indeed the case for the isolated molecules and, likewise, for CH_3I molecules inside He droplets. However, as for iodobenzene, the alignment of the molecules in the He droplets appears to be weaker than of the isolated molecules.

B. Alignment dependence on intensity

Having demonstrated that molecules in He droplets can be adiabatically aligned, an important question to consider is to which degree they can be aligned. For this purpose, the information provided by the ion images is quantified by determining the average value of $\cos^2\theta_{2D}$, $\langle\cos^2\theta_{2D}\rangle$, where θ_{2D} is the angle between the YAG pulse polarization and the projection of an I^+ or IHe^+ ion velocity vector on the detector screen, and plotting it as a function of the YAG pulse intensity I_{YAG}.

For the isolated diiodobenzene molecules $\langle\cos^2\theta_{2D}\rangle$ was determined for the radial range pertaining to only the outermost or the innermost Coulomb explosion channel, respectively, as well as for the radial range pertaining to both Coulomb explosion channels—the yellow circles in Fig. 2, row (a), indicate the radial ranges used. The results, displayed in Fig. 3(a), show that for the isolated $C_6H_4I_2$ molecules $\langle\cos^2\theta_{2D}\rangle$ rises from 0.5, the value characterizing a sample of randomly oriented molecules, at $I_{YAG} = 0$ to 0.95 for the outer (green squares) channel, 0.89 for the inner (blue diamonds) channel, and 0.91 for both channels (black squares) at the highest value of I_{YAG}. The $\langle\cos^2\theta_{2D}\rangle$ values are higher in the outer ring because the axial recoil approximation is better met for I^+ ions recoiling from a higher charged $C_6H_4I_2$ cation. Furthermore, the highest charge states of $C_6H_4I_2$ are formed in the volume of the probe laser focus where its intensity is highest, which is also the volume where I_{YAG} is highest and, thus, where the molecules are best aligned. Again these findings are fully consistent with previous results [23].

For the molecules in the He droplets $\langle\cos^2\theta_{2D}\rangle$ was calculated for the radial range encompassing the single radial channel observed. The velocity of the IHe^+ fragments is an intermediate of the velocity of I^+ from the inner and outer channel in the gas phase image. Thus, the single channel presumably corresponds to an average of the inner and outer channel observed in the gas phase. Assuming the same

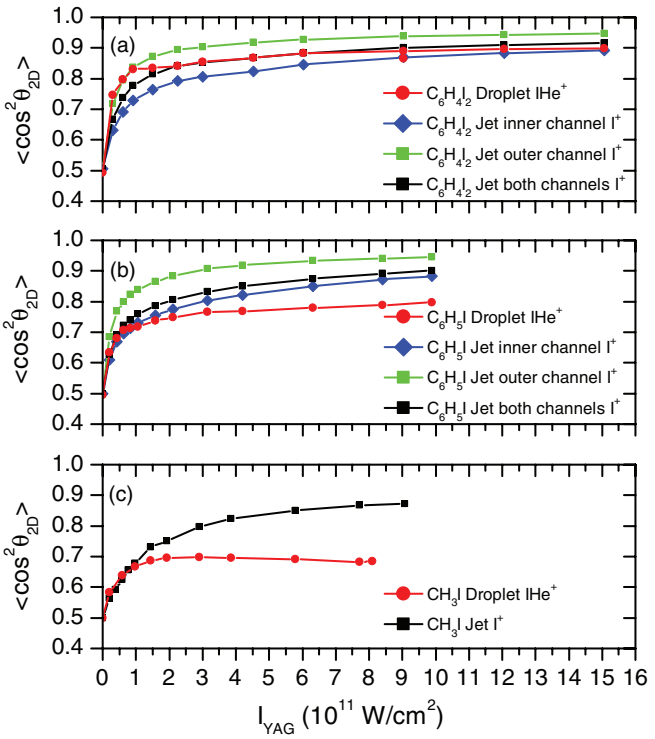

FIG. 3. (Color online) $\langle\cos^2\theta_{2D}\rangle$ recorded at different intensities of the YAG pulse for (a) diiodobenzene, (b) iodobenzene, and (c) methyliodide. Results for isolated molecules are shown by green squares and blue diamonds and results for molecules in He droplets by red circles.

branching ratio, this droplet value can be directly compared to the value obtained for both Coulomb explosion channels in the isolated molecule case for a quantitative comparison of the degree of alignment. It is seen that the degree of alignment of $C_6H_4I_2$ molecules in He droplets (red circles) is higher than in the gas phase (black squares) for $I_{YAG} < 2 \times 10^{11}$ W/cm^2 and the same (within experimental accuracy) for higher I_{YAG}. We conclude that adiabatic alignment of 1,4 diiodobenzene molecules in He droplets is essentially as efficient as for isolated molecules.

In the case of isolated iodobenzene molecules $\langle\cos^2\theta_{2D}\rangle$ was also determined for the radial range pertaining to the two individual Coulomb explosion channels as well as for the radial range pertaining to both the Coulomb explosion channels. For iodobenzene molecules in He droplets the radial range containing the single distinct Coulomb explosion channel was used. For the isolated molecules [Fig. 3(b)] the results are very similar to the $C_6H_4I_2$ results with $\langle\cos^2\theta_{2D}\rangle$ rising from 0.5 at $I_{YAG} = 0$ to 0.94 for the outer (green squares) channel, 0.88 for the inner channel(blue diamonds), and 0.90 for the joint channels (black squares) at the highest value of I_{YAG}. These findings are fully consistent with previous results [23]. For C_6H_5I molecules in He droplets $\langle\cos^2\theta_{2D}\rangle$ also increases as a function of I_{YAG} and the curve (red circles) in Fig. 3(b) closely follows the curve for the two Coulomb explosion channels in the gas phase up to $I_{YAG} = 1 \times 10^{11}$ W/cm^2, but falls below for higher I_{YAG}. In particular, the maximum $\langle\cos^2\theta_{2D}\rangle$ value at the highest YAG pulse intensity is 0.78.

For methyliodide the single Coulomb explosion channel, observed both for the isolated molecules and the molecules in He droplets, is used to determine $\langle\cos^2\theta_{2D}\rangle$. Qualitatively, the trend of the $\langle\cos^2\theta_{2D}\rangle$ curves [Fig. 3(c)] is similar to that observed for iodobenzene. The values obtained for both isolated and solvated CH_3I are, however, lower than the corresponding values for C_6H_5I, which is due to the lower polarizability anisotropy of CH_3I. For $I_{YAG} < 1 \times 10^{11}$ W/cm^2, $\langle\cos^2\theta_{2D}\rangle$ is about the same for isolated and solvated CH_3I. At higher YAG pulse intensities $\langle\cos^2\theta_{2D}\rangle$ continues to rise to the final value of 0.87 in the gas phase. For the droplet case the maximum $\langle\cos^2\theta_{2D}\rangle$ value is 0.68. At the highest YAG pulse intensities a minor decrease of $\langle\cos^2\theta_{2D}\rangle$ is observed. This is ascribed to an additional IHe^+ signal, induced by the combined action of the YAG and the probe pulse which increases as I_{YAG} is increased. These IHe^+ ions contribute to the Coulomb explosion channel at the highest I_{YAG} values and they reduce $\langle\cos^2\theta_{2D}\rangle$ because their emission direction is almost isotropic. For isolated molecules this effect also leads to a reduction of $\langle\cos^2\theta_{2D}\rangle$ at high YAG intensities.

IV. DISCUSSION

For a sample of isolated molecules, for simplicity treated as linear rigid rotors, the degree of adiabatic alignment is solely determined by the anisotropy parameter $\sqrt{\Delta\alpha I/4B}$ and the reduced rotational temperature kT_{rot}/B, where $\Delta\alpha$ is the polarizability anisotropy, I the intensity of the laser pulse, and B the rotational constant [1,25]. The intensity of the YAG pulse inside the He droplets is expected to be the same as outside and recording the saturation behavior (Fig. 3) ensures that the lower degree of alignment in the droplets, observed for iodobenzene and methyliodide, is not due to a weaker alignment field. The minor shifts of electronic transitions observed in spectroscopy of molecules in helium droplets imply that the polarizabilities are essentially identical to those of isolated molecules [18,19]. The rotational constants are expected to be lower by a factor of 3–5 in the droplet [18–20] and $T_{rot} = 0.38$ K is lower than for the isolated molecules by about the same factor [23]. This results in about the same reduced rotational temperature (kT_{rot}/B) for isolated and solvated molecules, while the anisotropy parameter should be higher in the droplet. Therefore, we anticipate that adiabatic alignment in the He droplets should be at least as strong as for the beam of isolated molecules. As shown in Fig. 3 this is the case for diiodobenzene but not for iodobenzene and methyliodode when $I_{YAG} \gtrsim 1 \times 10^{11}$ W/cm^2.

To unravel whether the lower degree of alignment detected in the He droplets results from (an unexpected) perturbation of the adiabatic alignment mechanism by the droplet in the iodobenzene and methyliodide cases, or from blurring of the initial emission direction of the Coulomb exploding ions due to the He environment, we studied the directionality of ions created by Coulomb explosion of unaligned molecules. The right column of Fig. 2 displays ion images recorded with the probe pulse only, now polarized in the detector plane. The gas phase images [rows (a), (c), and (e)] show that the probe pulse preferentially explodes molecules with the C-I axis localized around its polarization axis. This orientational selectivity of the probe process should also apply to the molecules inside He droplets and imply that the initial angular distribution of the Coulomb exploding ions is the same as for isolated molecules. For diiodobenzene in He droplets, row (b), the angular distribution of the ions is essentially the same as for the isolated molecules. For iodobenzene, row (c), and methyliodide, row (e), the angular distribution of ions from the molecules in the He droplets is broader and less confined than for the ions from the isolated molecules. This demonstrates that for CH_3I and C_6H_5I the initial directionality of the ions is lowered due to the helium environment. Consequently, the $\langle\cos^2\theta_{2D}\rangle$ values measured, and displayed in Fig. 3, underestimate the true degree of alignment of the CH_3I and C_6H_5I molecules inside the droplets compared to the isolated molecule case.

To identify the reason for the blurring of the initial ion emission anisotropy we recorded ion images with the probe pulse only for different ion species (IHe_n^+, $n = 0,1,2,\ldots$) and for different droplet sizes. No dependence on these parameters was observed and we conclude that by contrast to observations for photodissociation of molecules in droplets into neutral fragments [26], the initial directionality is not significantly blurred as the ion travels out of an intact droplet, for the droplet sizes studied here, but rather as a result of the Coulomb explosion inside the droplet. A Coulomb explosion of molecules in droplets creates not only ionic fragments from the molecule, but also many He_n^+ ions, which are not observed when probing the undoped droplet beam. In fact, the dominant He_2^+ signal is an order of magnitude larger than the I^+ signal. The He_n^+ ions from the doped droplets can be formed via field ionization by the strong static field from ionized molecules in combination with the laser field, or via a resonant absorption of an electronic nanoplasma driven by the intense laser pulse as investigated for clusters of rare gas atoms in droplets [27,28]. These He_n^+ ions create a charge distribution around the iodobenzene or methyliodide molecule which may not be symmetric with respect to the C-I bond axis. The resulting electrostatic repulsion between the He_n^+ ions and the I^+ ion, as it leaves the parent molecule, may cause the observed deviation from C-I axial recoil in the iododobenzene and methyliodide cases. The creation of an asymmetric (not cylindrical symmetric) charge distribution around the C-I bond axis should also cause a significant deviation from axial recoil for diiodobenzene molecules embedded in the He droplets, which is, however, not observed. This may be due to the higher symmetry of diiodobenzene (D_{2h}) as compared to iodobenzene (C_{2v}) and methyliodide (C_{3v}). In particular, the inversion symmetry of the molecule may suppress the formation of an asymmetric charge distribution.

The deviation from axial recoil implies that the probe pulse introduces a blur in the measurement of the alignment distribution. The blur will cause the largest relative deviation of the measured from the real spatial orientation when the molecules are strongly aligned. This is precisely what we observe: The $\langle\cos^2\theta_{2D}\rangle$ values for the molecules in the droplets are quite similar to the $\langle\cos^2\theta_{2D}\rangle$ values for the isolated molecules at low I_{YAG}, where the alignment is modest, but as I_{YAG} is gradually increased, and the alignment gradually grows stronger, $\langle\cos^2\theta_{2D}\rangle$ for the droplet molecules becomes increasingly weaker compared to $\langle\cos^2\theta_{2D}\rangle$ for the isolated molecules.

We note that control of the spatial orientation of molecules inside He nanodroplets has been addressed previously in the context of pendular state spectroscopy. It was shown that a strong static electric field (∼tens of kV/cm) can induce orientation of polar molecules in He droplets, i.e., force the dipole moments of the molecules to point in a particular direction [29–31]. The orientation results from the interaction between the permanent dipole moment of the molecule and the static electric field. This differs from the current work where the alignment results from the induced dipole moment and the electric field from the YAG pulse. As such a laser pulse cannot by itself create orientation but the axial confinement, i.e., the 1D alignment it induces, is much sharper than what can be obtained by the strong static field. Moreover, for rotationally cold or, better, quantum state-selected, isolated molecules a moderately intense laser field can create strong alignment and orientation simultaneously if combined with a weak static electric field [32–34]. It may be possible to transfer this combined fields effect to molecules embedded in He droplets.

V. CONCLUSION

In conclusion, we have presented experimental results showing that moderately intense laser pulses can create strong 1D adiabatic alignment of molecules dissolved in He droplets. For low I_{YAG} the alignment of all three molecules under study is at least as good as for the isolated molecules under identical laser conditions. In the high intensity limit, in the case of diiodobenzene the degree of alignment equals that of isolated molecules in a rotationally cold (∼1 K) beam under identical laser conditions, whereas in the case of iodobenzene and methyliodide it is weaker. We believe that the Coulomb explosion probe method underestimates the degree of alignment in the droplets as compared to the gas phase due to a (stronger) deviation from axial recoil. Alternative probe schemes such as photodissociation [26] and linear dichroism [35,36] may provide more quantitative information about the true degree of alignment.

We expect that 3D alignment of molecules inside He droplets—potentially for a broad range of molecular sizes and classes—can be achieved by replacing the linearly polarized alignment pulse with an elliptically polarized pulse, just as for isolated molecules [37]. Such fixed-in-space molecules could be very useful for a variety of studies including time-resolved imaging of molecular frame reactions in the presence of a dissipative media and structural determination by diffraction [38]. The strong adiabatic alignment may be rendered field free by rapidly truncating the pulse at its peak. In the gas phase field-free alignment immediately following turn-off only persists for a few hundred fs due to rapid dephasing associated with free molecular rotation [39,40]. For molecules inside He droplets we recently showed that field-free alignment generated by a subpicosecond laser pulse persists for 5–10 ps. Thus, an alignment pulse adiabatically turned on and nonadiabatically turned off [41] may be a versatile approach to obtain molecules that are tightly aligned inside He droplets under field-free conditions for times sufficiently long to follow chemical transformations through their entire duration.

ACKNOWLEDGMENT

The work was supported by the Danish Council for Independent Research (Natural Sciences), The Lundbeck Foundation, and the Carlsberg Foundation.

[1] B. Friedrich and D. Herschbach, Phys. Rev. Lett. **74**, 4623 (1995).
[2] T. Seideman, J. Chem. Phys. **103**, 7887 (1995).
[3] W. Kim and P. M. Felker, J. Chem. Phys. **104**, 1147 (1996).
[4] H. Sakai, C. P. Safvan, J. J. Larsen, K. M. Hilligsøe, K. Hald, and H. Stapelfeldt, J. Chem. Phys. **110**, 10235 (1999).
[5] H. Stapelfeldt and T. Seideman, Rev. Mod. Phys. **75**, 543 (2003).
[6] J. Itatani, J. Levesque, D. Zeidler, H. Niikura, H. Pépin, J. C. Kieffer, P. B. Corkum, and D. M. Villeneuve, Nature (London) **432**, 867 (2004).
[7] C. Z. Bisgaard, O. J. Clarkin, G. Wu, A. M. D. Lee, O. Gessner, C. C. Hayden, and A. Stolow, Science **323**, 1464 (2009).
[8] D. Shafir, H. Soifer, B. D. Bruner, M. Dagan, Y. Mairesse, S. Patchkovskii, M. Y. Ivanov, O. Smirnova, and N. Dudovich, Nature (London) **485**, 343 (2012).
[9] L. Holmegaard, J. L. Hansen, L. Kalhoj, S. Louise Kragh, H. Stapelfeldt, F. Filsinger, J. Kupper, G. Meijer, D. Dimitrovski, M. Abu-samha, C. P. J. Martiny, and L. Bojer Madsen, Nat. Phys. **6**, 428 (2010).
[10] J. L. Hansen, J. H. Nielsen, C. B. Madsen, A. T. Lindhardt, M. P. Johansson, T. Skrydstrup, L. B. Madsen, and H. Stapelfeldt, J. Chem. Phys. **136**, 204310 (2012).
[11] J. Ohkubo, T. Kato, H. Kono, and Y. Fujimura, J. Chem. Phys. **120**, 9123 (2004).
[12] S. Ramakrishna and T. Seideman, Phys. Rev. Lett. **95**, 113001 (2005).
[13] S. Ramakrishna and T. Seideman, J. Chem. Phys. **124**, 034101 (2006).
[14] T. Vieillard, F. Chaussard, D. Sugny, B. Lavorel, and O. Faucher, J. Raman Spectrosc. **39**, 694 (2008).
[15] N. Owschimikow, F. Königsmann, J. Maurer, P. Giese, A. Ott, B. Schmidt, and N. Schwentner, J. Chem. Phys. **133**, 044311 (2010).
[16] D. Zhdanov and H. Rabitz, Phys. Rev. A **83**, 061402 (2011).
[17] J. M. Hartmann and C. Boulet, J. Chem. Phys. **136**, 184302 (2012).
[18] J. P. Toennies and A. F. Vilesov, Angew. Chem., Int. Ed. **43**, 2622 (2004).
[19] F. Stienkemeier and K. K. Lehmann, J. Phys. B **39**, R127 (2006).
[20] M. Y. Choi, G. E. Douberly, T. M. Falconer, W. K. Lewis, C. M. Lindsay, J. M. Merritt, P. L. Stiles, and R. E. Miller, Int. Rev. Phys. Chem. **25**, 15 (2006).
[21] D. Pentlehner, J. H. Nielsen, A. Slenczka, K. Mølmer, and H. Stapelfeldt, Phys. Rev. Lett. **110**, 093002 (2013).
[22] J. J. Larsen, H. Sakai, C. P. Safvan, I. Wendt-Larsen, and H. Stapelfeldt, J. Chem. Phys. **111**, 7774 (1999).
[23] V. Kumarappan, C. Z. Bisgaard, S. S. Viftrup, L. Holmegaard, and H. Stapelfeldt, J. Chem. Phys. **125**, 194309 (2006).

[24] For the rightmost images in rows (a) and (b), $I_{\text{probe}} = 1.0 \times 10^{14}$ W/cm^2.
[25] B. Friedrich and D. Herschbach, J. Phys. Chem. A **99**, 15686 (1995).
[26] A. Braun and M. Drabbels, J. Chem. Phys. **127**, 114303 (2007).
[27] A. Mikaberidze, U. Saalmann, and J. M. Rost, Phys. Rev. Lett. **102**, 128102 (2009).
[28] S. R. Krishnan, L. Fechner, M. Kremer, V. Sharma, B. Fischer, N. Camus, J. Jha, M. Krishnamurthy, T. Pfeifer, R. Moshammer, J. Ullrich, F. Stienkemeier, M. Mudrich, A. Mikaberidze, U. Saalmann, and J.-M. Rost, Phys. Rev. Lett. **107**, 173402 (2011).
[29] K. Nauta, D. T. Moore, and R. E. Miller, Faraday Discuss. **113**, 261 (1999).
[30] K. Nauta and R. E. Miller, Science **283**, 1895 (1999).
[31] L. Pei, J. Zhang, and W. Kong, J. Chem. Phys. **127**, 174308 (2007).
[32] B. Friedrich and D. Herschbach, J. Chem. Phys. **111**, 6157 (1999).
[33] H. Sakai, S. Minemoto, H. Nanjo, H. Tanji, and T. Suzuki, Phys. Rev. Lett. **90**, 083001 (2003).
[34] L. Holmegaard, J. H. Nielsen, I. Nevo, H. Stapelfeldt, F. Filsinger, J. Küpper, and G. Meijer, Phys. Rev. Lett. **102**, 023001 (2009).
[35] F. Dong and R. E. Miller, Science **298**, 1227 (2002).
[36] W. Kong, L. Pei, and J. Zhang, Int. Rev. Phys. Chem. **28**, 33 (2009).
[37] J. J. Larsen, K. Hald, N. Bjerre, H. Stapelfeldt, and T. Seideman, Phys. Rev. Lett. **85**, 2470 (2000).
[38] J. C. H. Spence and R. B. Doak, Phys. Rev. Lett. **92**, 198102 (2004).
[39] J. G. Underwood, M. Spanner, M. Y. Ivanov, J. Mottershead, B. J. Sussman, and A. Stolow, Phys. Rev. Lett. **90**, 223001 (2003).
[40] M. Muramatsu, M. Hita, S. Minemoto, and H. Sakai, Phys. Rev. A **79**, 011403 (2009).
[41] S. Guérin, A. Rouzée, and E. Hertz, Phys. Rev. A **77**, 041404(R) (2008).